

Contents lists available at [SciVerse ScienceDirect](http://www.elsevier.com/locate/jas)

Journal of Archaeological Science

journal homepage: <http://www.elsevier.com/locate/jas>

Prospects and problems in the use of hyperspectral imagery for archaeological remote sensing: a case study from the Faynan copper mining district, Jordan

Stephen H. Savage^{a,*}, Thomas E. Levy^b, Ian W. Jones^b

^aArchaeological Research Institute, School of Human Evolution & Social Change, Arizona State University, 951 S. Mill Ave., Box 872402, Tempe, AZ 85287-2402, United States
^bDepartment of Anthropology and Center of Interdisciplinary Science for Art, Architecture, and Archaeology, UC San Diego, United States

ARTICLE INFO

Article history:

Received 10 July 2011
 Received in revised form
 22 September 2011
 Accepted 23 September 2011

Keywords:

Hyperion
 Iron age copper mining
 Jordan
 Spectral mixture analysis
 Principle components analysis

ABSTRACT

Hyperspectral (multiple, narrow band) satellite imaging provides a useful discovery and analytical tool for archaeologists. The Hyperion instrument, flying on the Earth Observer 1 (EO-1) satellite, was launched from Vandenberg Air Force Base on November 21, 2000. Unlike 7-band Landsat or 15-band ASTER imagery, Hyperion provides 242 (196 calibrated) narrow bands in the visible (VIS) to shortwave infrared range (SWIR), enabling much more detailed archaeological and geological analyses. It was designed as a spectrometer specifically geared to mineralogical analysis, and the imagery is freely available via data acquisition (targeting) requests from NASA. We requested a Hyperion image swath targeted on Khirbat en-Nahas (KEN), an ancient copper smelting site along the Wadi al-Ghuwayb (WAG), a part of Jordan's Faynan district, where extensive ore processing occurred from the 3rd millennium BCE to industrial scale production over several centuries in the early 1st millennium BCE (Iron Age) and continued until Medieval Islamic times. We use a combination of Principal Components Analysis (PCA), similarity matrices, and Spectral Mixture Analysis (SMA) on a single image swath to help locate additional ore processing sites, distinguish different areas at KEN that drew on different ore deposits, and discern depositional differences that may help illuminate issues related to the organization of production at KEN. Extensive field surveys in the research area provide a unique opportunity to 'ground-truth' the results of the hyperspectral research. The results of our study show considerable promise for future work with Hyperion data sets, and illuminate new aspects of the copper smelting industry at Khirbat en-Nahas. However, the low spatial resolution of the imagery and the nature of weakly reflective bands in the near infrared (NIR) limit the utility of the results.

© 2011 Elsevier Ltd. All rights reserved.

1. Introduction

Where satellite remote sensing has been used in archaeological research, it has most often utilized imagery from sources such as Landsat, ASTER, SPOT, and CORONA. A wide range of work shows the utility of these well-known resources; some of them have been applied to ancient mining and smelting sites. Derooin *et al.* (2011) used visible and SWIR bands from a time series of Landsat imagery to identify gossans (iron caps) possibly related to archaeological remains in the Jabali region of Yemen. Pryce and Abrams (2010) attempted to use ASTER imagery to identify control signatures for known prehistoric copper smelting sites in Thailand, but issues of scale, chemistry, and vegetation limited their success.

The use of hyperspectral imagery is less well known. Traviglia (2006) experimented with the MIVIS (Multispectral IR and Visible Imaging Spectrometer) airborne instrument in the region around

Aquileia, Italy. Applying a wide range of analytical techniques to the image product, Traviglia noted a number of problems, including "resolution, atmospheric corrections, noise reduction, and post-processing issues such as redundancy of data and the large number of images to handle..." (2006: 123). In spite of these issues, the MIVIS data "provide considerable support in identification of features in the non-visible domain and [was] demonstrated to be a valid instrument for archaeological research..." (2006: 129–130). Parcak (2009:101–102) lists only three studies, all using data from airborne spectrometers; since then, two additional studies have been published using space-borne sensors. Kwong *et al.* (2009) used hyperspectral classification and unmixing in support of an ongoing archaeological study in the Oaxaca Valley of Mexico with the aim of better understanding soil and vegetation types related to ancient settlement and trade systems. However, they emphasize the need for ground-truth studies of their results.

The use of space-based hyperspectral platforms, such as NASA's Hyperion instrument, originally developed especially for geological and mining applications, has only recently begun to be explored.

* Corresponding author. Tel.: +1 480 727 0858; fax: +1 480 965 7671.
 E-mail address: shsavage@asu.edu (S.H. Savage).

Alexakis et al. (2009) used data from four sensors, including Hyperion, to detect settlements and validate the results of GPS surveying in a low relief region in Greece where hundreds of Neolithic settlements/tells were established from the Early Neolithic period until the Bronze Age (6000–3000 BC).

Our study illuminates a number of possible methods and avenues of archaeological research with this freely-available data source, but points to the need for some element of ground-truthing and the desirability of higher resolution imagery.

The study presented here was constructed as a double-blind analysis of the copper mining region in the Faynan district of southwestern Jordan (Fig. 1). This area has been intensively studied by archaeologists since the early 1980s (e.g., Barker et al., 2007; Hauptmann, 2007; Levy et al., 2008). Savage uses a variety of methods, including Principal Components Analysis (PCA), construction of similarity matrices, and spectral mixture analysis of geologically-based end members to examine a Hyperion image that includes the Iron Age copper smelting site of Khirbat en-Nahas. Savage, who conducted the analysis of the satellite imagery, has never been to the site. Levy has limited background in satellite remote sensing, but has worked in the Faynan region of Jordan since 1997 and is able to provide critical ground-truthing expertise against which the image analysis can be juxtaposed. Jones, a student of Levy's, performed image cross-checking against real-world survey results from the research area.

Following brief descriptions of the history of archaeological research, in the Faynan district of Jordan, its basic geology, and of the EO-1 satellite and Hyperion instrument, we report a method for atmospheric correction of Hyperion data, results of PCA to search for

spectral signatures that indicate smelting sites, the creation of a similarity matrix based on slag mounds from Khirbat en-Nahas, and spectral mixture analysis of geologically-based end members. These analyses point to areas where additional smelting sites may be located, and demonstrate that Hyperion data can help distinguish subdivisions at the site level where unique spectral signatures indicate different sources of copper ore may have been processed. Our results demonstrate some of the capabilities of using these multispectral data for further archaeological research. However, the results are limited by the weakly reflective near IR bands, and by the relatively low resolution (30 m) of Hyperion imagery.

2. Archaeological research in the Faynan district

Since 2002, the University of California, San Diego's Levantine Archaeology Laboratory has spear-headed an interdisciplinary field investigation of the role of mining and metallurgy in Iron Age (ca. 1200–500 BCE) societies who resided and exploited copper ore in Jordan's Faynan district. The work is conducted in collaboration with Dr. Mohammad Najjar, formerly Director of Excavations and Surveys of the Department of Antiquities of Jordan (DOAJ).

The Iron Age coincides with the rise of the first local historic state-level societies in this part of the southern Levant. As Faynan contains the largest concentration of copper ore deposits in the southern Levant it played a key role in the social and economic fabric of societies who interacted with this region during the late second and early first millennium BCE (Levy, 2009). However, there are copper ore sources throughout the Arabah Valley with the second largest concentration located in the south in the Valley (Rothenberg, 1999). Consequently, our research has been drawn into a wide range of anthropological, historical, ancient technology and research methodology debates. The new excavations and surveys carried out by our team both embellish and add new perspectives concerning Iron Age copper production in the southern Levant. A summary of the Iron Age work carried out by our team is presented elsewhere (Levy et al., in press).

The earliest researchers in Faynan, such as Musil (1907), Frank (1934) and Glueck (1935) carried out brief field surveys in the Faynan region and provided mostly descriptive reports of the archaeological remains. Most of this work done in the first half of the twentieth century used a literal approach to the Judeo-Christian Biblical sources. Archaeological surveys carried out in the 1970s and 1980s were not focused specifically on the Iron Age or Faynan, but did touch on these subjects (MacDonald, 1992; Raikes, 1980). The first surveys that focused specifically on Faynan were carried out as part of a multi-period archaeometallurgical study in this part of the southern Levant by the Deutsches Bergbau-Museum (DBM) during the 1980s and early 1990s (Adams, 1991; Hauptmann, 2007). This pioneering work laid the foundation for all later science-based archaeological research in the Faynan region. Since this study was aimed specifically at understanding the history of mining and metallurgical technology, its surveys and excavations focused only on metallurgical contexts such as mines and smelting sites. Non-metallurgical archaeological sites such as cemeteries, roads, non-metal producing settlements, irrigation networks, agricultural field systems and other sites were not accounted for to the same extent. While the basic assemblages of copper production and technologies were reported, the socio-historical role of mining and metallurgy in the societies that lived in Faynan was not investigated in depth. Small scale excavations were carried out at several Iron Age sites during the DBM project (Fritz, 1994, 1996), but the fieldwork was fast-paced with little in-depth analyses. Thus, historical interpretations made by Biblical scholars attached to the GMM project were highly speculative, based, as they were, on very incomplete archaeological data.

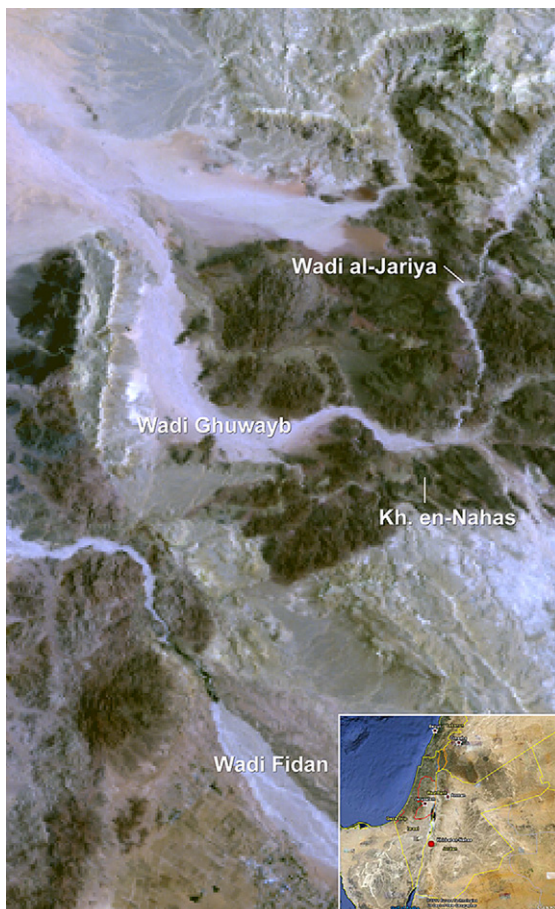


Fig. 1. The western part of the Faynan district covered by the Hyperion image.

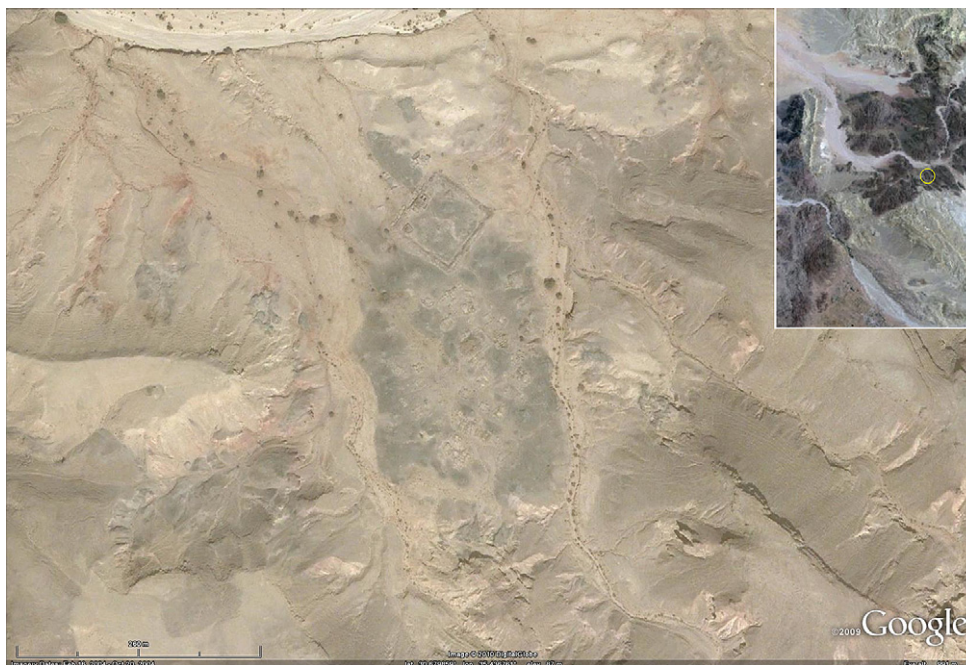


Fig. 2. Google Earth image of Khirbat en-Nahas. The dark gray areas are slag mounds; the square structure is an Iron Age fortress. The right inset shows the Hyperion study area, with the site circled in yellow. (For interpretation of the references to color in this figure legend, the reader is referred to the web version of this article.)

A more social perspective on the Iron Age archaeology in Faynan began in 1995 with the Wadi Faynan Landscape Survey, carried out by the Council for British Research in the Levant (CBRL). This project was primarily aimed at understanding deep-time processes of desertification spanning the Holocene rather than a focus on Faynan's ancient metallurgy in anthropological perspective (Barker et al., 2007; Mattingly et al., 2007). Important and innovative studies concerning ancient pollution and the paleoenvironment were carried out by this team; some were related to the Iron Age (Grattan et al., 2007; Pyatt et al., 1999). While the survey results and methodologies applied are excellent, the lack of excavations carried out in conjunction with the intensive surveys in the main Faynan valley system make it difficult to date field systems tied to specific periods.

UCSD's Edom Lowlands Regional Archaeology Project (ELRAP) is an outgrowth of the Jabal Hamrat Fidan (JHF) project that since 2003 has focused primarily on intensive surveys along a number of the main drainage systems and large-scale excavations related to the Iron Age of the Faynan region. The last year of the JHF project focused on the first large-scale excavations at Khirbat en-Nahas (KEN; Arabic = ruins of copper) – the largest Iron Age copper production site in the southern Levant (Figs. 2 and 3, Higham et al., 2005; Levy et al., 2004, Levy et al., 2005a, b). The spectacular nature of the discoveries at and around KEN, including extensive and detailed evidence for copper smelting over a 10 ha area, one of the largest Iron Age fortresses in the desert region of southern Jordan, Israel and Sinai, deep stratigraphy at the site and the abundance of related Iron



Fig. 3. Overview of the Iron Age (ca. 1200–900 BCE) copper production site of Khirbat en-Nahas, southern Jordan. Extensive black 'slag mounds' indicate ancient smelting of copper ore mined locally (Photo: T E L, UCSD Levantine Archaeology Laboratory).

Age sites in the surrounding area, led us to establish ELRAP with its Iron Age focus. In 2006, the second large-scale excavation campaign was carried out at KEN that focused on systematically excavating one of the deeply stratified 'slag mounds' at the site and other areas (Levy et al., 2008). A sondage was also made that season at Khirbat al-Jariya, a second tier Iron Age copper production site located upstream from KEN (Ben-Yosef et al., 2010). We also surveyed and probed one of the Iron Age fortresses located high above the Wadi al-Ghuwayb near extensive mine complexes. In 2009, large-scale excavations were resumed at KEN completing the first phase of our investigations at the site. That season was also an opportunity to make a sounding at the newly discovered Iron Age Jabal al-Jariya (JA) mines (Ben-Yosef et al., 2009) and the previously unexcavated settlement/production site of Khirbat al-Ghuwayba. Taken together, these surveys, large-scale excavations and probes coupled with a program of rigorous radiometric dating has provided an unprecedented Iron Age database for investigating cultural and technological change in ancient Edom.

ELRAP has become a test bed for cyber-archaeology, (the cybernetics of archaeology, referring to all the interconnective relationships which the datum produces, the code of transmission, and its transmittability; see Forte, 2010) and a wide range of digital methodologies for archaeological field research. As the Iron Age of Edom is so closely linked to issues concerning the relationship between ancient texts and the archaeological record, the project has been at the forefront of applying high-precision radiocarbon dating to the historical archaeological record. Taken together, our robust methodology that combines cyber-archaeology and high-precision radiometric dating coupled with Bayesian analyses provide a model for how Biblical (or other historical) archaeologies can explore the relationship between ancient text and the archaeological record today (Levy et al., 2010). This new methodology has changed not only the Iron Age chronology of Edom, but opened the door to new social, cultural and technological interpretive models for this key period helping to stimulate scholarly debate (Finkelstein, 2005; Finkelstein and Piasezky, 2006, 2008; Finkelstein and Singer-Avitz, 2009; Levy, 2005, 2008, 2010; Levy and Higham, 2005a, 2005b; Levy and Najjar, 2006; Levy, Najjar, and Higham et al., 2005a5; van der Steen and Bienkowski, 2006).

3. Geology of the Faynan district

The Faynan district is located in southwestern Jordan, between north latitudes 30–31 and east longitude 35–36; Faynan is part of the Wadi Araba rift system, which is a northern extension of the great East African Rift Valley. Rabb'a (1994) presents a detailed description of the geology of the Faynan district, which is only touched upon here; Hauptmann (2007) provides a more general description. Here we present a short discussion drawn from their publications to orient the reader to the principal, relevant geological formations.

Strike-slip movements along the Araba rift, which began in the Cenozoic, have displaced the Faynan about 100 km northward from the geologically identical Timna region, located west of the rift system in Israel. The copper ores in both regions belong to the family of stratiform, sedimentary rock-hosted copper deposits. The copper mineralization (mostly chrysocolla, with malachite, paratacamite, cuprite, and minor chalcocite) is bound in strata a few meters thick found in flat-lying arkosic sandstone, dolostone, and shale (Lehmann, 2008:456).

The rocks that crop out in the study area comprise the Aqaba and Araba (basement) Complexes and various sedimentary cover rocks. The igneous rocks comprise caic-alkaline plutonic granitoids and acidicbasic volcanics cut by multiple dyke swarms. The Aqaba Complex of Late Proterozoic to Early Cambrian age, is represented by the As Sadra Granodiorite, the Hunayk Granodiorite, the

Minshar Granite and the Ghuwayr Volcanic Suite. It displays the characteristic peneplaned upper surface overlain by sediments of the Ram Group. The Araba Complex comprises the Ahaymir Volcanic Suite and the Finan Granitic Suite. The sedimentary cover rocks comprise the Lower Palaeozoic Ram Group, the mesozoic Kurnub Sandstone Group, the marine Ajiun and Belqa groups (mesozoic-cenozoic), and Neogene to Recent sediments.

The Aqaba and Araba Complexes form part of the crystalline basement of the Arabian Shield, that is interpreted to be made up of a series of accreted terrains, dominated by ensimatic arcs but including at least one micro-continental terrane, that were swept together and collided with cratonic Africa during the final stages of the Pan African orogenic cycle. Following this arc-continent collision event widespread, related, granitoid magmatism took place throughout the composite Arabian-Nubian Shield. Sedimentation through the Early Paleozoic, Mesozoic and Cenozoic was essentially controlled by eustatic and tectonic fluctuations of the Arabian-Nubian Shield (ANS), the influence of the Tethys Ocean and the development and tectonics of the Dead Sea Transform Fault System (Rabb'a 1994: 1).

According to Rabb'a (1994:47), "Copper mineralization is present in the volcanic acidic rocks of the Ahaymir Suite as crusts



Fig. 4. Geology of the Faynan Region (from Rabb'a 1994). HK – Hunayk Monzogranite, FN – Feldspar Porphyry, BDS – Burj Dolomite-Shale, IN – Umm Ishrin Sandstone, KS – Kurnub Sandstone.

infilling joints but the main Cu-ore targets are in the sedimentary rocks unconformably overlying the basement Araba complex units." Rocks of the Ahaymir Suite are not indicated in the study area, though they do occur as a broad southwest to northeast trending band a few kilometers southeast of the study area.

"The second most common occurrence is present in the Burj Dolomite–Shale (BDS) Formation which comprises three members from base to top, the Tayan Siltstone, Numayri Dolomite and Hanneh Siltstone. The most important member for copper mineralization is the Numayri Dolomite, which is about 40 m thick" (Rabb'a 1994:47). The Burj Dolomite Shale formation consists of two siliclastic members separated by a carbonate member. The lowest member comprises green, red- brown and buff micaceous siltstone and (very) fine-grained sandstone. The middle member consists of carbonates which comprise yellow-brown or gray, dolomitic limestone, dolomite and sandy dolomite with sandstone lenses; ooids and peloids are present. There are often thin beds of micaceous siltstone intercalated in this part. The upper member consists of siltstone and sandstone intercalated with thin beds of fine to medium grained sandstone, rich in Cu mineralization (Rabb'a 1994: 19). BDS occurs in large deposits north of the Wadi al-Ghuwayb, on both sides of its tributary, the Wadi al-Jariya, and in isolated pockets south of the Wadi al-Ghuwayb (Fig. 4)

4. The Earth Observer 1 (EO-1) satellite and the Hyperion instrument

The NASA EO-1 satellite was launched on November 21, 2000 on a one-year technology validation/demonstration mission. The EO-1 spacecraft flies three primary instruments, of which the Hyperion is the first high spatial resolution imaging spectrometer to orbit the earth. Hyperion has 242 spectral bands in the range .4 μm –2.5 μm , in the Visible (VIS) and Short Wave Infrared (SWIR) ranges.¹

¹ The bands are .001 μm wide and the instrument's signal to noise capabilities are sufficient to resolve many of the finer features that such spectral data can bring to remote sensing. The instrument records data in 7.7 km wide swaths, approximately 100 km long, with 30 m nominal ground resolution. LAC is an imaging spectrometer covering the spectral range from 900 to 1600 nm, used by the EO-1 Science Validation Team to monitor the atmospheric water absorption lines for correction of atmospheric effects in multispectral imagers. (<http://edcscns17.cr.usgs.gov/eo1/sensors.php> retrieved October 26, 2010). The EO-1 satellite has a 10:00 AM mean local time (MLT) equatorial crossing on a north-south, sun-synchronous path; the initial repeat was 16 days. Upon its launch, EO-1 followed the same orbital path as Landsat, but 1 min behind it. However, EO-1 no longer follows the Landsat 7 satellite. It left the Landsat 7 path in October 2007 when NASA began lowering its orbit to its required re-entry altitude, in order to stay within the 25 year re-entry limit called for in the NASA orbital debris guide. NASA planned on lowering the orbit in steps to use the rest of the fuel while maintaining the 10:00 AM MLT crossing. In July 2008 NASA requested and was granted an orbital debris waiver because the science team thought that lowering the orbit further would degrade the science; since EO-1 was still viable, they were granted the waiver. Subsequently NASA has maintained the satellite in a 705 × 685 km orbit and using its remaining fuel to perform maneuvers to adjust the orbit so it can stay at 10:00 AM MLT equatorial crossing without going any lower (Frye, 2010a). The EO-1 Extended Mission is chartered to collect and distribute ALI multispectral and Hyperion hyperspectral products in response to Data Acquisition Requests (DARs). Under the Extended Mission provisions, image data acquired by EO-1 are archived and distributed by the USGS Center for Earth Resources Observation and Science (EROS) and placed in the public domain. Imagery from Hyperion can be acquired at no cost from NASA/USGS, via DARs and downloads. Data are delivered via FTP pull. The Hyperion data products consist of 242 channels (bands) in hdf or geotiff format (one geotiff image for each band); the hdf product is not georeferenced, and some georeferencing inaccuracies have been observed in the geotiff product, which require subsequent correction. Of the 242 instrument bands, 196 are the primary useable ones. The reduction from 242 to 196 bands resulted partly because a number of the detectors on the instrument were "not illuminated" in the detector arrays and partly because there is a region of overlap in the VNIR and SWIR detector arrays (Jupp, 2001:4). The Level 1 data provided to the public reports radiance at the sensor adjusted for gain and offset values (Pearlman, 2003; Ungar, 2010).

We requested a targeted Hyperion image from NASA, in the Faynan region of southwestern Jordan, and it was acquired Wednesday August 11, 2010 at 11:12:40. Of the 196 calibrated bands, 40 others exhibit considerable streaking, caused by calibration differences in the detector array, which vary according to ground and atmospheric conditions (Goodenough et al., 2003: 1322–1323). This left 156 viable bands for the present analysis. We used the Davinci software application to process the Hyperion data swath.²

5. Atmospheric correction of Hyperion imagery

The Level 1 data from Hyperion are not atmospherically corrected.³ Since atmospheric correction was needed to pursue additional analysis of the imagery, we applied a form of dark-object subtraction on the data to correct it.

Electromagnetic radiation from the sun is measured at the Hyperion sensor after passing through the atmosphere, reflecting from the surface of the earth, and passing through the atmosphere again to strike the sensor. During that journey, portions of the total radiance are absorbed, so that only a percentage of the original radiance is returned to the sensor. In addition, photons strike molecules in the atmosphere (chiefly water vapor, dust, smoke, and other pollutants) and scatter, meaning that not all the EM radiation reaching the sensor originated by reflecting from the part of the surface being imaged. Consequently, the image may appear brighter than it actually is. The scattering is most pronounced in the blue end of the spectrum.

Commercially available image processing software frequently has an atmospheric correction algorithm built in; such routines typically make use of a kind of generic atmosphere model, based on northern hemisphere values at mid latitudes in the summer, with an assumed humidity level of about 40%. It can be argued that these conditions are frequently not met, especially in the arid regions of the Middle East. Atmospheric conditions vary continuously everywhere on earth. So a scene-based method is desirable. The Davinci program does not have a native atmospheric correction algorithm, but dark-object subtraction is a straightforward process using Davinci commands.

On the moon, ground that is in shadow appears black, because EM radiation from the sun is blocked by the object casting the shadow and there is no atmosphere to scatter light into the shadowed region. But the Hyperion sensors record a non-zero value in shadowed places on earth, and it can be assumed that the

² Davinci is a free, open source application developed at the Mars Space Flight Facility, School of Earth and Space Exploration, Arizona State University. The application runs under Windows and UNIX, and can be downloaded from <http://davinci.mars.asu.edu/index.php>. In addition, we used Global Mapper to create image overlays; in each the end product of various steps in Davinci was added as one or more layers to three visible light bands of the Hyperion image.

³ NASA currently provides atmospheric correction of Hyperion imagery based on atmospheric modeling by request, and the product is delivered in the .hdf (non-georeferenced) data format. Thus, the researcher must choose between non-atmospherically corrected, georeferenced imagery and corrected non-georeferenced imagery. We chose the latter option and applied our own atmospheric correction methods. Information from the Linear Etalon Imaging Spectrometer Array (LEISA) Atmospheric Corrector, which also flies on EO-1 and captures atmospheric data while Hyperion gathers multispectral data (Ungar et al., 2003) can theoretically be used, but additional work is needed to perfect the method, and then the backlog of existing imagery will be corrected (Frye, 2010b). When all of the image analysis is scene-based, and confined to a single Hyperion image as we do here, pre-processing image correction procedures are not strictly necessary. However, if the researcher wishes to combine adjacent image swaths (these are taken on different days, with different atmospheric conditions), or conduct SMA using an end-member library derived from lab spectra (see Clark et al., 2007) then atmospheric correction and other corrective measures are required. (Khurshid et al. (2006).

difference between zero and the value observed in a shadow is the result of scattering. Chavez (1988) developed a method for scene-based correction of Landsat 5 imagery based on five different atmospheric models. Prior to Chavez's work, a histogram method was used to detect a sharp increase in the number of pixels at some non-zero DN (digital number—the value in the band image, which can range from 0 to 255). It was assumed that the sharp increase at this non-zero value represented the amount of atmospheric scattering, and the values of the total image were adjusted downward by subtraction. Chavez pointed out that this method can overcorrect because the values selected across all the bands may not conform to a realistic relative atmospheric scattering model (1988:466). His improved method used several atmospheric models to scale the amount of subtraction across Landsat bands. However, when we attempted to apply this method by expanding the atmospheric models to account for the 196 bands of calibrated Hyperion data, we found that it also overcorrected in longer wavelengths.

Instead of applying one subtraction value to all the bands as was done prior to Chavez's work, or overcorrecting based on an expanded application of his method, we chose to apply the dark object subtraction method to each band individually, following Vincent and Beck (2005). With the help of Christopher Edwards, a Research Associate at the Mars Space Flight Facility, we developed a histogram subtraction function in Davinci that can process the entire Hyperion image cube by iterating through the bands and performing an automated dark object subtraction on each band that requires it.

6. Principal components analysis and the search for ore processing sites

The slag mounds at Khirbat en-Nahas are easily seen in the visible light bands of the Hyperion image; the mounds at the site are large, spread over a substantial area, and stand out prominently from the surrounding surfaces. Other ore processing sites in the region are not as large, and hence, not as easy to see in the visible satellite image. But there may be other band combinations beyond the visible spectrum that can make such places stand out. Unfortunately, image display is limited to three bands at a time, represented as blue, green and red to form a full color image. Taken three bands at a time, with 156 bands there would be 620,620 possible combinations to examine, clearly an impractical process. Furthermore, there is frequently an excessive amount of interband correlation—where images generated by different band combinations appear very similar. Principal Components Analysis (PCA) comes to the rescue here. PCA is a dimension reduction technique that preserves the variability in the original dataset; it addresses both of these issues.

In PCA, the original n -band dataset is compressed into fewer than n "new bands," where each new band or principal component is orthogonal to every other. The new image data derived from a PCA are linear combinations of the original data values multiplied by the appropriate transformation coefficients, or eigenvectors (Lillesand et al., 2008:527–533). The vast majority of the variance in the original image (sometimes greater than 95%) is captured by the first principal component, and each subsequent component contributes less and less. The PCA reduces the interband correlation and the number of bands required to see virtually all the variation in the original dataset. The transformation can be applied to enhance visual interpretation of the scene or as a way to increase the computational efficiency of automated classification procedures. PCA has been used successfully in several archaeological remote sensing applications (see Parcak, 2009:97–99).

A PCA was performed on the 156 good bands from the Hyperion image with Davinci. Fig. 5 illustrates a portion of the study area (enlarged for later discussion) showing the first component as blue, the second as green, and the fourth as red. Together, these three components encompass 98.75% of the variance in the original 156 bands. Khirbat en-Nahas clearly stands out as a group of orange pixels of different intensities against a background of different shades of green; it is the area shown in the white rectangle near the bottom center of the figure.

Several other regions that have a similar appearance have been outlined in white on the PCA image. There are a number of them north of Wadi al-Ghuwayb and others on the east side of Wadi al-Jariya, in areas where ELRAP conducted ground surveys in 2002 and 2007. Comparison of the survey results with the PCA image can help to determine if the indicated areas are false positives, whose spectral similarity to the slag mounds at KEN is caused by other factors than ore processing. Two of the areas identified as hotspots in the PCA image are very close to the recently discovered Jabal al-Jariya (JAJ) pit mine fields north of Wadi al-Ghuwayb (Fig. 5a and b; Ben-Yosef et al., 2009). These possibly represent outcrops of minerals similar to those in the slag at KEN, although the mines themselves are not identified on the image due to the nature of the pit mine field, discussed later in this paper. Likewise, two orange areas at the right edge of the image correspond to a large set of mostly Iron Age mines in the southern Wadi al-Jariya mining district, identified during the 2002 survey of Wadi al-Jariya (Fig. 5c and d; Levy et al., 2003; Knabb et al., in press.). Another orange area to the east of KEN is associated with WAG 57, a primarily Middle Islamic mining site, and WAG 58, a smaller Iron Age and Middle Islamic mining site, both of which were identified during the 2002 Wadi al-Ghuwayb survey (Fig. 5e; Levy et al., 2003; Knabb et al. in prep.). To the southwest of KEN is another hotspot, associated with another set of Iron Age mines (Fig. 5f; Hauptmann, 2007:128–129). This represents all of the major mine clusters which have been identified during surveys of Wadi al-Ghuwayb and Wadi al Jariya, and PCA seems to be a useful tool for directing surveys toward these large-scale features in the landscape.

One of the largest hot spots on the image, however, does not seem to correspond to any feature associated with mining or metallurgy (Fig. 5g). This is located in a patch of Hunayk Monzogranite, and no mining or smelting sites were found here during the Wadi al-Jariya survey, although the major Iron Age smelting site of Khirbat al-Jariya lies ca. 800 m to the north (Levy et al., 2003). Additionally, Khirbat al-Jariya itself does not show up as an obvious hotspot on the image, although smelting certainly took place there during the Iron Age, perhaps because it is significantly smaller than KEN. The false positives, and the false negatives for smelting sites, are significant limitations of the PCA method as applied to survey. But it is important to emphasize again that for clusters of mines few false negatives were encountered in this analysis. As such, PCA is a valuable tool for planning ground surveys of mining districts.

While geological surveys have been carried out in the region, there are always unknowns. A case in point is the recent discovery of relatively extensive field of Iron Age pit mines approximately 1 km northwest of KEN that are now called the Jabal al-Jariya (JAJ) mines (Ben-Yosef et al., 2009). While conducting a survey for ancient roads, hundreds of shallow plate-like depressions ranging 1.5–3 m in diameter were found that are identical to similar pit mines found in the southern Arabah valley at Timna (Ben-Yosef et al., 2009; Conrad and Rothenberg, 1980). The mines penetrated into colluvial deposits that contained copper nodules eroded from the Cambrian ore-bearing Burj formation. As Ben-Yosef et al. (2009:100) point out, a post-Precambrian magmatic plug that extends for about 1.5 km, is the only Phanerozoic magmatism known in the Faynan region and may imply that the richness of the

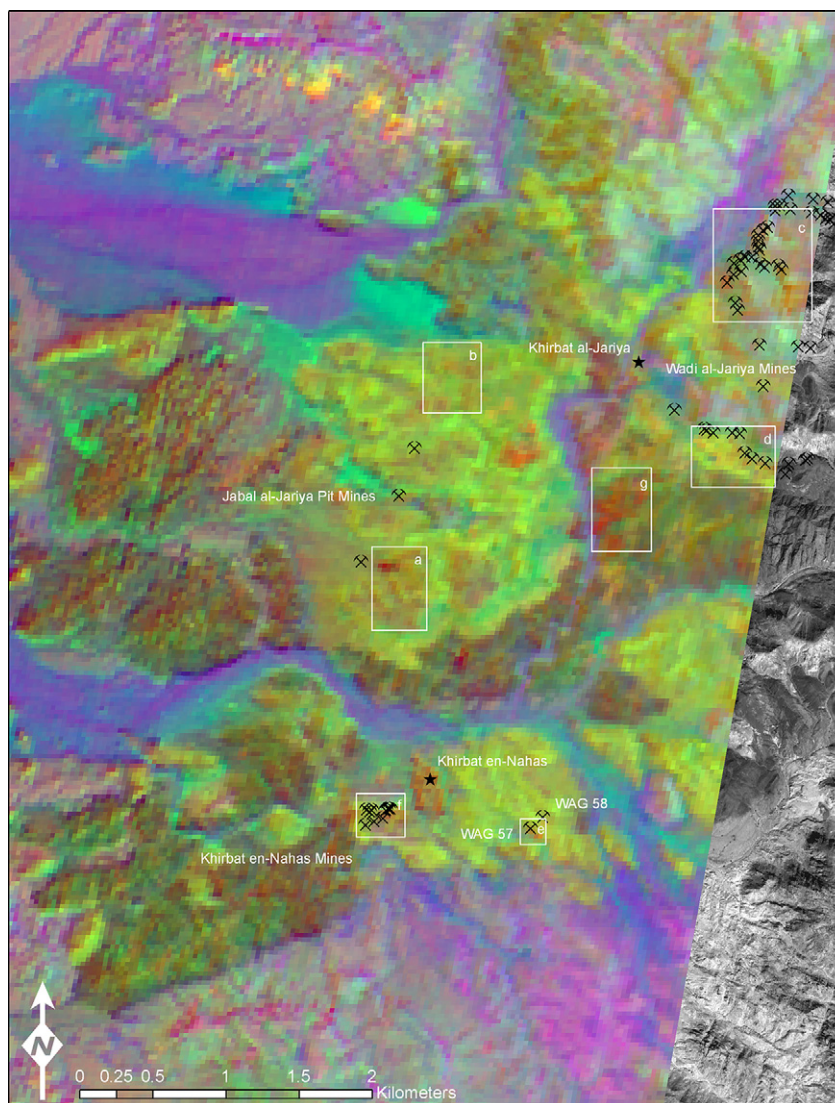


Fig. 5. Results of principal components analysis on the Hyperion image cube, showing the site and areas with similar spectral signatures. Lower case letters refer to areas discussed in the text.

copper mineralization in this specific locale was influenced by this magmatic feature (e.g., Segev and Sass, 1989). The discovery of the JAJ mine field in the Faynan district was completely fortuitous and suggests that 'hotspots' similar to those identified in Fig. 5 be 'ground truthed' in the near future for evidence of ore or metallurgical activities. In addition, many of the Iron Age copper mines in the region start at the surface as shafts dug through overbearing rock layers down to the interface with the copper ore-bearing BDS layer, and then proceed to excavate galleries along the interface to extract the copper ores. This procedure would create a mixed spectral signature from mining debris, which would include components from the overlying rock and the BDS formation. So areas that do not appear on the geology map in Fig. 4 as BDS may have a partial BDS signature as a result of mining activity.

The PCA procedure has been a useful exercise, in that it has shown us where there are other potential ore processing sites. Our results suggest that, while this method seems to be successful in identifying some mining areas, traditional ground-based surveys must be employed as well to distinguish false positives from areas with actual ancient copper exploitation, and to find sites too small to be detected reliably by Hyperion. But it is a useful prospecting

method when combined with field survey, and PCA is a valuable tool for reduction of redundant information across multiple image bands, and it can help accentuate features that are invisible to the human eye (see Traviglia, 2006: 126). In our case, however, the resolution of Hyperion imagery renders the results less than optimal. The issue here is not with the method per se, but with the fact that in the Faynan region many of the features we would like to identify are too small to be seen in the coarse resolution of Hyperion images. Traviglia (2006: 124) found that even the 3–4 m resolution of the MIVIS airborne instrument was too coarse for some archaeological purposes. But we feel that it is important to include PCA in our image processing toolbox, since in other regions and applications archaeologists may be able to locate larger features than we have attempted. In addition, the PCA procedure has illuminated differences in the spectral signatures among the various pixels at KEN that represent slag mounds, indicating that the different mounds have different geological mixtures, which means that materials at different places of the site have originated in different locales in the region. These observations can be more fully addressed by constructing similarity matrices and spectral mixture analysis, to which we now turn.

7. A similarity matrix for Khirbat en-Nahas Slag Mounds

The extensive copper smelting operations at KEN, which took place over several centuries in the early 1st millennium BCE, have left significant slag mounds on the surface of the site (Figs. 2 and 3). The PCA procedure described above has indicated other areas in the region that may have been ore processing loci. A closer examination of the pixels that represent KEN shows different color values (shades of orange) indicated in areas of the site represented by different slag mounds, and at the various hotspots discussed above. It would be useful to determine whether there are other pixels in the Hyperion image cube that have a very similar spectral signature to specific pixels at the site, as they would indicate areas where ores were extracted and processing activities are more likely to occur.

In order to accomplish this, a similarity matrix was created for several different pixels at KEN, using Davinci. We read in all the calibrated bands from the Hyperion swath and concatenated them into an image cube, which is essentially a three-dimensional array of numbers ranging from 0 to the maximum value recorded at the sensor. The X and Y dimensions of the cube correspond to 30 m pixels on the ground, and the Z dimension represents the values in the various Hyperion bands. This process results in a very large data structure, and we trimmed out the northern and southern sections of the image bands in order to preserve computer memory for subsequent processing.

Using any visible band, we can identify the pixels in the X and Y directions that represent the slag mounds at KEN. Then, examining the Z values for those locations through the Z dimension of the image cube provides a spectrographic profile of a pixel representing a slag mound. The image cube must be normalized for each pixel being inspected (in order to compensate for albedo effects). Following normalization, for each pixel under study we created a second three-dimensional result array the same size as the original image cube, and set all its values to zero; then we iterated through the normalized image cube one band at a time, looking at the Z values at each X/Y location to see if they are equal to the Z value at the slag mound location for that band. If they are equal, we placed a 1 in the result array for that X/Y location and Z band. Once the result array was built, we simply collapsed it to an X/Y array of only one band, by adding the values of the Z dimensions for each X/Y location. The end result was a two-dimensional array with values ranging from 0 to 156 (the number of original bands in the image cube), where higher values indicate places with greater spectrographic similarity to the slag mound locations.

Fig. 6 illustrates the similarity matrices for six loci at KEN that represent slag mounds. For each locus, we present only those places in the rest of the study area where the similarity index is greater than 100, that is, where at least 100 bands in the Hyperion image cube have values identical to those at one of the slag mounds at the site. Most of the high similarity regions are located north of the site, across Wadi al-Ghuwayb and up the Wadi al-Jariya; though there are also a number of similar pixels in the region of the Khirbat en-Nahas mines southwest of the main site.

The similarity matrix only identifies places where 2/3 of the values in the Hyperion image are the same. It does not specify which values are the same, so some locations might be similar in bands that are not indicative of ore processing. Since the slag at KEN rests on Salib Arkosic Sandstone deposits in the Wadi Fidan, and not on materials where copper ores originated in the Faynan district (Rabb'a 1994), they are the product of human transportation and deposition. Thus, locations with high similarity values that also occur on geological deposits that do not bear copper ores may be postulated to be the result of smelting activity. When highly similar areas correspond to copper-bearing rock formations, then it is possible that potential sources for the ores processed at KEN have

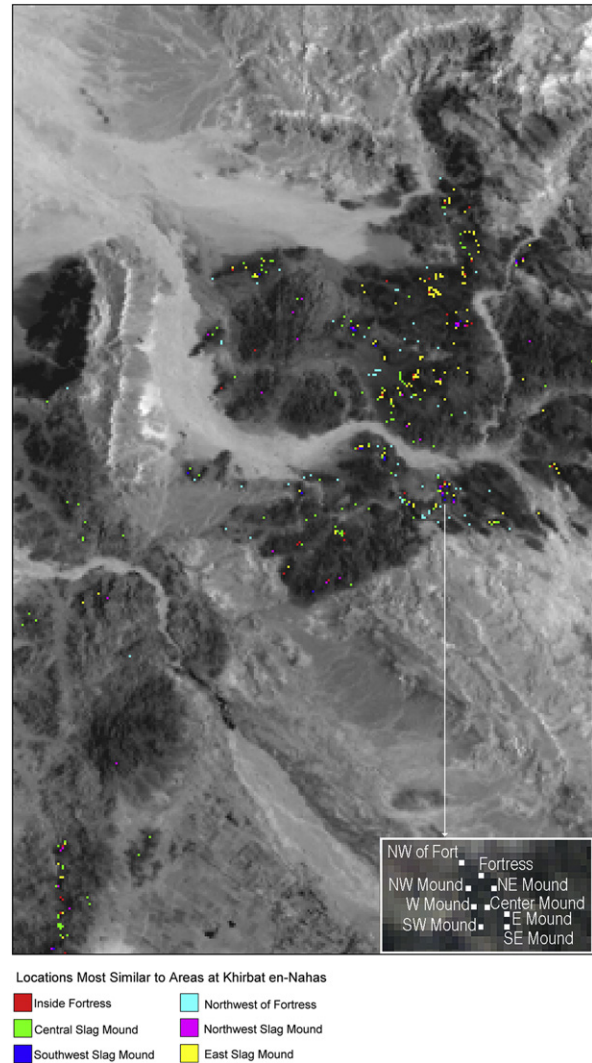


Fig. 6. Areas most similar to six slag mound pixels at Khirbat en-Nahas.

been identified. In terms of ground truth, the similarity matrix picks up the mapped concentrations of the main copper ore-bearing deposit in the region – the Burj Dolomite-Shale unit, and in particular, the northern portion of the Wadi al-Jariya where over 70 mines have been found (Levy et al., 2003; Knabb in prep). However, the similarity matrix also highlights areas dominated by different kinds of granite, which indicates that the slag mounds contain mixed spectral signatures. We will use spectral mixture analysis below to unmix these areas.

8. Spectral mixture analysis

One drawback to conventional classification methods, whether unsupervised or supervised, is that they divide an image, pixel-by-pixel, into discrete classes. Since the slag deposits at KEN exhibit different spectral signatures, and there are known copper mines throughout the study area (as indicated on Fig. 5) the ores processed at different locations at KEN may have originated in a number of different, mixed ore deposits, which may have come from any combination of the mineral hotspots in the region. Thus, simply subdividing the image through standard classification methods is insufficient to the case.

Instead of placing each pixel in an image into one of a set of discrete classes, spectral mixture analysis (SMA) starts with a set of

end members, representing a spectral library, and then deconvolves the image through linear unmixing to reveal the percentages of end members present in each pixel analyzed.

The fundamental principle of this technique is that the emitted or reflected energy from a multimineralic surface is a decipherable combination of the energy radiated from each component in proportion to its areal percentage. For the assumption of linearity with respect to spectral mixing, the areal percentage of surface minerals (end members) with known particle sizes and densities translates into the volume present. If spectra of pure end members are known, mixed spectra can then be deconvolved through a least squares linear fit resulting in a percentage of each input end-member plus several measures of the model quality. In mineralogy, an end-member is at the extreme end of a mineral series in terms of purity. Deconvolution provides a relatively straightforward and computationally quick method of assessing the mineral assemblages of a surface, thereby reducing hyperspectral data sets to a minimum informational volume. In addition, the products of such an analysis (areal percentage, end-members present, and model error) are easier to interpret, especially where translated into an image format, than are thermal radiance values or arbitrarily classified pixels (Ramsey and Christensen, 1998: 577).

The SMA procedure was developed for deconvolution of thermal IR imagery (Ramsey and Christensen, 1998). However, in SWIR bands, the linear assumptions that underlie SMA are not met. With the weaker near IR bands, small particles of opaque materials can have a disproportionately large effect on the deconvolution result set (Salisbury and Wald, 1992:124–126; Moersch and Christensen, 1995:7473–7476). The Davinci SMA routine allows the mixture of end members present to be rounded to the nearest five percent, and we report those rounded values in Table 1 below for each of the deconvolved loci at the site. But we adopt a more conservative approach in our subsequent discussion, and treat the mixtures as presence/absence indicators when discussing constituents, and only relative amounts where the same constituents are seen in more than one slag mound.

From Ramsey and Christensen's discussion it is clear that identification of end members is critical to the SMA operation. In this case, we used the geology map published by Rabb'a (1994) to identify fifteen end members, based on the major classifications provided on the map. Since we sought to perform the analysis to determine the constituents at KEN and the large mineral hotspots none of these areas were used as end members. Furthermore, end-member locations from the map were chosen as much as possible in the center of large, homogenous regions (shown in Fig. 7 as red squares with abbreviations from Rabb'a 1994). While it can be argued that any geological formation chosen as an end-member is itself a mixture of components, so that an SMA produces mixtures that are percentages of percentages, identifying end members in

the center of large, apparently homogenous regions from the geology map will tend to minimize this effect.

Two strengths in using hyperspectral data in an SMA are the potential for including a large spectral library of end members and the fine resolution of the EM frequency curve (because of the narrow bandwidth of each band and the continuous coverage). Neither Landsat nor ASTER imagery provides the large number of narrow, continuous bands that render SMA analysis useful in hyperspectral image analysis. The SMA analysis allows $n-1$ end members to be used, where n is the number of bands in the image. The six bands of Landsat or the 15 bands of ASTER severely limit the potential of the SMA procedure. Furthermore, the bandwidths in Landsat and ASTER are too wide for effective analysis, since they result in very coarse model results.

8.1. SMA at Khirbat en-Nahas—Composition of the slag mounds

As shown in Figs. 2 and 3, Khirbat en-Nahas is covered with extensive mounds of slag and ancient metallurgical debris related to smelting activities during the Iron Age. Stratigraphic excavations and a major radiocarbon dating project at the site demonstrate that industrial scale metal production took place during the 10th and 9th c. BCE followed by the total abandonment of the site. We wanted to examine the Hyperion imaging of this smelting center to see if any variability could be detected. SMA Deconvolution of the center slag mound at KEN is shown in Fig. 8.

Khirbat en-Nahas contains over 21 slag mounds, which have different spectral signatures and probably contain the detritus from different sources of ore and metallurgical activities (furnace

Table 1
Results of spectral mixture analysis of Khirbat en-Nahas slag mounds.

Mound	End members and percentages present ^a
Northwest mound	BDS 90%, Plg2 10%
Northeast mound	BDS 95%, MM 5%, Plg2 <5%
East mound	BDS 100%
Southeast mound	BDS 100%
Southwest corner	BDS 75%, MM 15%, GR 5%, HK 5%
West mound	BDS 95%, Plg2 5%
Center mound	BDS 50%, Plg2 30%, HK 15% SB 10%
Fortress	BDS 90%, Plg2 10%, MM <5%
NW of Fortress	BDS 85%, AL 10%, Als 5%, MM <5%

^a Rounded to nearest 5%; total may exceed 100%.

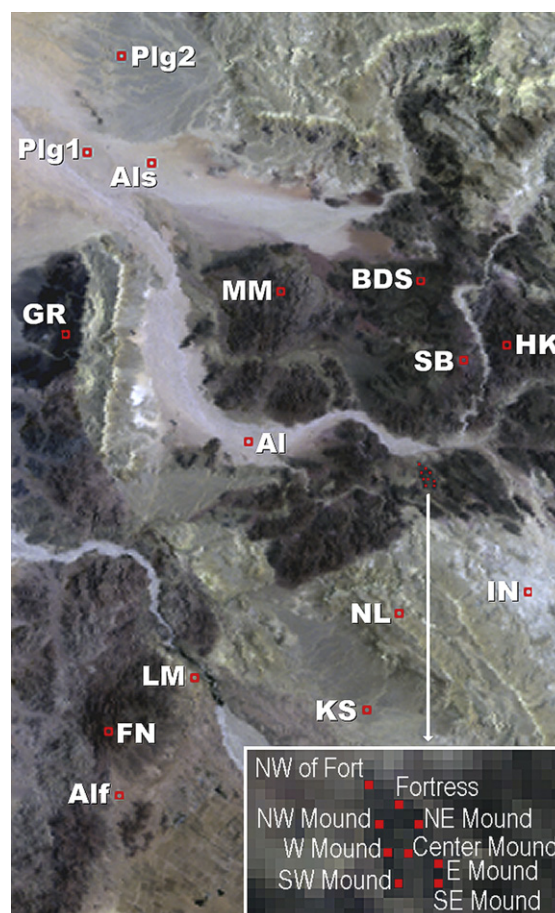


Fig. 7. Location of scene-based end members based on Rabb'a (1994).

fragments, tuyère pipes, features, etc.). We conducted an SMA on pixels that represent six of the main slag mounds at the site. Table 1 summarizes the results.

The SMA study clearly indicates that the various slag mounds visible in the Hyperion imagery have different spectral compositions representing different parent end-member mixtures, possibly from different sources. This suggests they may have been loci of different activities at the site, and indicates that some areas may have been more intensively used for ore processing than others (for example, the east and southeast mounds which have only BDS present). Whether the mounds represent smelting activity that occurred at different times, or smelting that was conducted at broadly similar times but by different groups remains an open question.

Burj Dolomite Shale dominates all the slag mound pixels tested, with the exception of the center mound. SMA indicates that the center slag mound is a mixture of four end members: Burj Dolomite Shale, Fluvial Gravel (Plg2), Hunayk Granodiorite (HK) and Salib Arkosic Sandstone (SB), which is the rock upon which Khirbat en-Nahas rests. BDS is the main constituent of the copper-bearing ores smelted at the site, and the components in the central slag mound suggest that BDS was obtained from regions with the other, non ore-bearing materials. Since the similarity matrix indicated that there were areas quite similar to the central slag mound located in HK rocks near the JAJ mines northwest of the site, the HK material found in the SMA analysis may have come from that area. Moreover, the HK deposits are found quite near Plg2 deposition, which may account for its presence in the deconvolution of the central slag mound. In the northern part of the site, the surface of KEN is made up mostly of Plg2. It is possible that the pixels analyzed for the northern slag mounds were slightly larger than the mounds themselves, and contain some mixture from this surface, as well.

The SMA results also indicate that activities other than ore processing may have occurred near the slag mound loci in different areas of the site. For example, the southwest slag mound contains a mixture of BDS, Minshar Monzogranite (MM), Ghuwayr Volcanic Suite (GR) and Hunayk Granodiorite (HK). Since these other components are not usually associated with ore processing at the site, other activities that resulted in their being imported to the site may be indicated, though a sample of the GR material was analyzed

at the Jordanian Natural Resources Authority and found to contain 1000 ppm copper (Rabb'a 1994:11). Only the southwest slag mound contains this material, and additional research is needed to understand the implications of its presence at Khirbat en-Nahas.

8.2. On the social relations of production at Khirbat en-Nahas

Our study provides intriguing insights into the possible organization of copper production in the Iron Age Faynan. If a single social group controlled access to the entire region's ore resources and to the entire processing site at KEN, then we might expect to see little or no difference in the spectral signatures of the various slag mounds. Under these social conditions, we might expect that ore from any mine might be processed at any locus at KEN, which would create a more or less homogenous spectral signature across the entire site, with SMA end members from each of the different ore sources found in relatively equal amounts in each of the slag mounds examined. The same situation could be expected to occur if different social groups controlled different ore sources, but the processing was organized and run as a single enterprise—we would see ores from any or all of the different sources distributed more-or-less evenly across the entire production site. However, if both the ore sources and the processing were differentially controlled, then we might expect to see different ore sources being processed in different places at the site. That a single, larger entity (as represented by the fortress) may have had overall control of the copper production does not preclude the possibility that production was organized as a group of parallel operations, each drawing from its own resources, since the organization could easily be horizontal at the lower level, yet feed into a more vertically oriented state-run operation.

The results of our studies with similarity matrices and SMA indicate that the six pixels analyzed have different spectral signatures, corresponding to different mixtures of geological end-members drawn from a variety of loci in the Faynan region. This suggests that a number of potentially independent ore processing operations, each with its own mines and smelting loci, operated at the site. However, because of the coarse resolution of the Hyperion imagery, we could not perform the analysis on each of the 21 major

Deconvolution of the Central Slag Mound at Khirbat en-Nahas

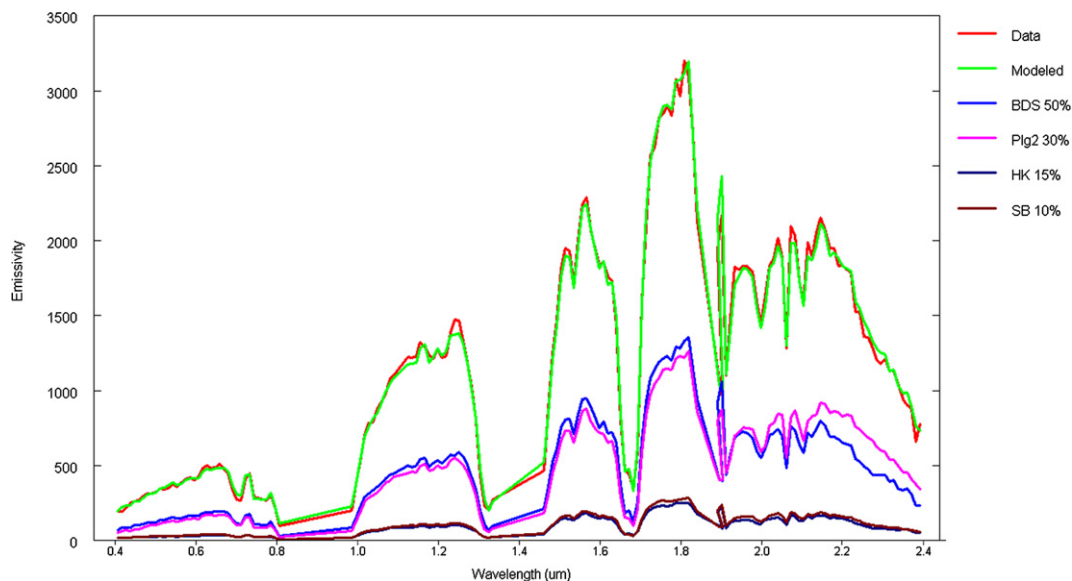


Fig. 8. Spectral Mixture Analysis Deconvolution of the Central Slag Mound at Khirbat en-Nahas.

slag mounds present at KEN because we cannot distinguish them in the image. Higher resolution imagery will help resolve these questions, which can be further addressed through excavations of a variety of the slag mounds, comparing the slag to the ore signatures.

9. Summary and evaluation

Hyperion imagery presents a new and useful resource to archaeologists. The preliminary studies reported here indicate that techniques such as PCA, similarity matrices, and SMA can provide much additional information that is of archaeological interest, opening up new avenues for potential research and investigation. Through these techniques we have shown where there are areas in the Hyperion image that may indicate additional ore extraction or smelting activities, and we have shown that the components of the slag mounds at Khirbet en-Nahas have different mixes of geological end members. That result suggests that different areas of the site were used to process ores from different sources, rather than all areas of the site being used to process ores from all of the different mines, which helps open up additional avenues of inquiry into the social relations of production in the Iron Age Faynan.

While this study has focused on metallurgy and the organization of production in the Faynan region of Jordan, its methods and techniques have broad application elsewhere. Hyperion is essentially a space-borne spectrometer, and has the potential to identify many different spectrographic signatures on earth, wherever there is sufficient ground exposure. Essentially, the result of any human activity that produces material remains with an identifiable

spectrographic signature at sufficient scale is amenable to analysis with Hyperion imagery. SMA and similarity matrices are especially useful tools, since they can use scene or lab-based end members for comparison. Geological end-member libraries (e.g. Clark et al., 2007) currently contain thousands of different mineral types, as well as specimens that are produced by people. Since any solid substance can be analyzed for its spectral signature, the potential uses are almost endless. As higher resolution instrumentation becomes available, we foresee greater potential for the use of hyperspectral image analysis in archaeological research. A researcher can identify a particular deposit by its spectrographic signature, and through the methods discussed here, use hyperspectral imagery as a prospecting tool, which would help direct ground survey and excavation. And once these methods are developed to the point where spectral mixtures can be discerned at different intra-site loci, as we have begun at KEN, then further insight into the organization of production can be gleaned from many different industries in different regions.

As promising as these results appear, though, there are a number of problems inherent in the Hyperion imagery that make it less than optimal for archaeological research. First, the resolution, at 30 m per pixel, is far too coarse to depict small features on the ground. Since mineshafts in the Faynan district tend to be fairly small – often less than 2 m in diameter – there would seem to be little hope of seeing them directly in a Hyperion image. Only if a large number of shafts were located within the same pixel on an image would we expect to be able to detect them visually. But we have shown that PCA is able to combine information from all available bands, while filtering out redundant values between

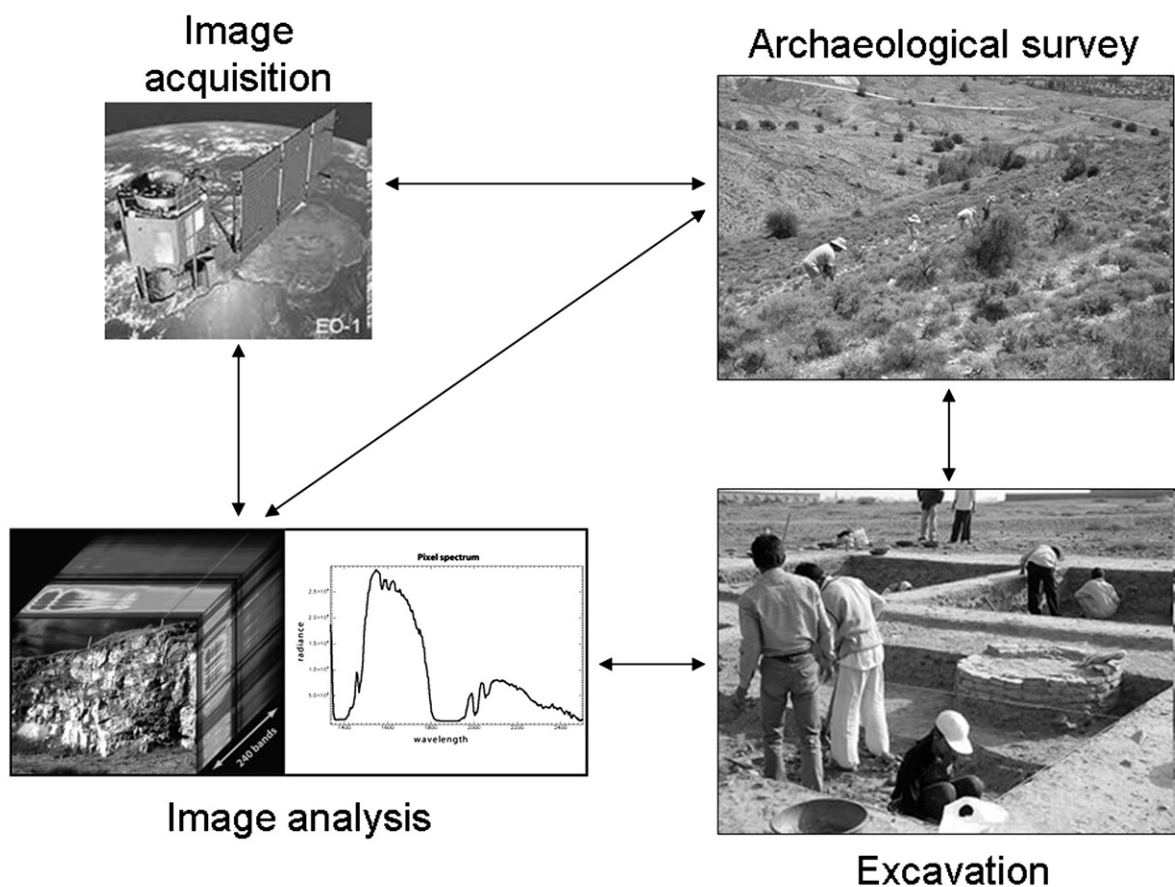


Fig. 9. Relationships among remote sensing and fieldwork operations.

bands, to produce a distribution of principal components that indicates where additional ore processing sites may be found. Clearly, PCA is not a substitute for ground-level archaeological survey, but it does point the archaeologist to places of interest; ground-truthing will be required to filter out the false positives and firmly identify the archaeological features.

Another difficulty with the Hyperion image is the weak nature of the SWIR bands the instrument covers. These reflected IR bands are subject to water absorption features and do not lend themselves to SMA as well as the stronger, thermal IR bands. We have shown that Davinci software can produce interesting results with SMA on the SWIR bands, but these results cannot be as rigorously interpreted as SMA with thermal bands. Taken simply as relative abundances with respect to SMA of different locations, and as presence/absence indicators for the end members at specific locations, though, we have shown that SMA can provide information about potentially different activities at various loci at KEN.

The relationships among image acquisition, analysis, and archaeological survey and excavation are complex (Fig. 9), and in any specific situation the entry point into the analytical path will vary depending on the nature and extent of prior knowledge of the region in question. In our case, many surveys and excavations had already been conducted in the Faynan region, so we already knew what we were looking for. Even so, our analysis produced unexpected results and suggests new avenues of inquiry. In areas that

are less well known, it might be best to start with high-resolution imagery, so that places of interest can be identified. At that point, a feedback relationship between ground truthing and hyperspectral image acquisition and analysis should be used to further refine areas for subsequent excavation and hypothesis testing. At any step, however, the archaeologist may find it desirable to revisit the analysis, acquire additional imagery, or conduct additional fieldwork. There is no set recipe other than to design the analysis and testing so that each stage can inform the others in a feedback mechanism.

Likewise, the particular steps involved in the image analysis will vary depending on the problems being addressed and the resources brought to bear (Fig. 10). In our case, we started with the site at KEN and requested a Hyperion image centered on it. Then, we clipped out a reasonable study area around the site and rotated it the image to eliminate the void areas caused by the satellite path angle relative to the equator. We eliminated the bad bands in the 242 received and performed dark object subtractions on the remaining 156 bands to correct for atmospheric EM scattering. PCA allowed us to condense more than 98% of the variability across these 156 bands into 3 bands that we combined in Global Mapper to produce the image shown in Fig. 5, and then we added known results from archaeological surveys to the image. This allowed us to evaluate the effectiveness of the PCA procedure. In other circumstances, these results might need to be ground truthed before additional analysis,

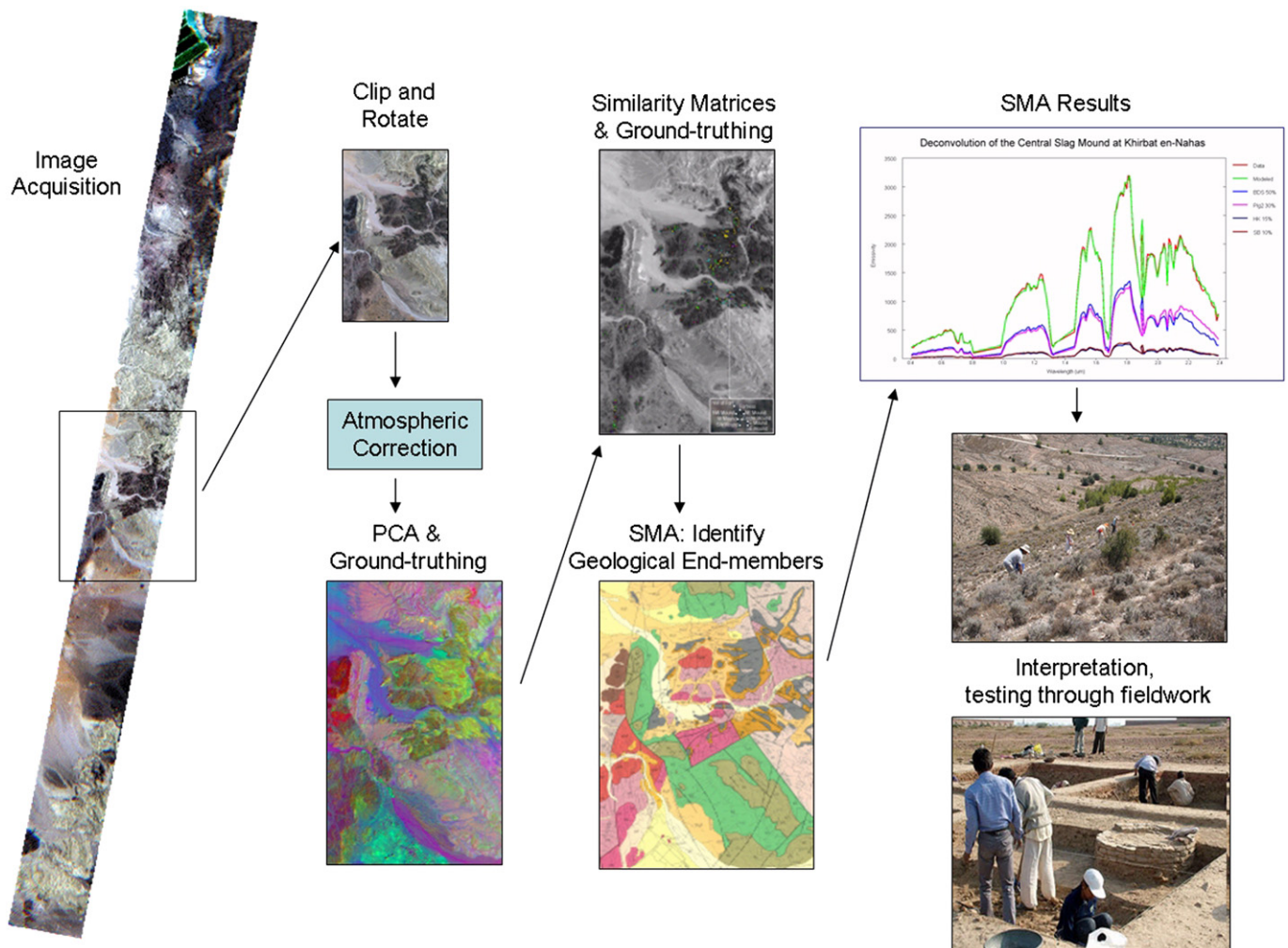


Fig. 10. Steps used in the analysis process.

but in our case the area had been “pre ground-truthed.” Further analysis of the PCA image indicated that there were differences in the spectrographic signatures of different parts of KEN that were not apparent from the visible light image. The similarity matrices we developed helped us understand that these areas at the site were more broadly similar to different pixels in the region, suggesting that ores and other materials were drawn from a variety of places, and utilized differently at the site. The SMA procedure confirmed and elaborated on these results, opening up new avenues of inquiry into the social relations of production at the site, which can be tested through additional fieldwork.

Higher resolution, hyperspectral, thermal IR band coverage would present better data for local-scale archaeological purposes. However, instruments in longer wavelengths require much larger receiving antennae and/or longer dwell times; increasing the spatial resolution has similar requirements. Creating the ideal instrument with thermal IR coverage, from 4 to 200 microns, for example, at 4 m spatial resolution would require a satellite beyond our current lift and financial capacity.

However, Hyperion data does provide a valuable resource for regional archaeological surveys, and especially for detection and initial classification of archaeo-metallurgical areas of interest. It can tell us interesting things about a landscape, and suggest places where archaeologists should conduct ground surveys. It can also raise interesting archaeological questions that touch on the social relations of production, but can only be answered with excavation. As an important new tool in the archaeologists’ cyber-dig bag, we have only scratched the surface of its potential application, and we look forward to NASA’s follow-up missions with instruments developed from the results of the EO-1 satellite.⁴

Acknowledgments

We express our thanks to several people at NASA, including Stuart Frye, Jay Pearlman, and Stephen Ungar, for their help in setting up a Hyperion data acquisition request, and answering many questions about the nature of the Hyperion data product. This study could not have been done without them. Thanks are also due to Alicia Rutledge and Christopher Edwards, Research Assistants at the ASU Mars Space Flight Facility, for introducing us to the Davinci software, and especially to Chris, who helped develop atmospheric correction and similarity matrix routines. We owe a great deal to Dr. Phil Christensen, for two semesters of graduate level remote sensing lectures, for explaining the intricacies of the Spectral Mixture Analysis routines in Davinci, and for reading and commenting on an earlier draft of the paper. Erez Ben-Yosef, Sidney Rempel, and Steven Schlich and also read earlier versions of the

⁴ As the EO-1 satellite is de-orbited the time when it crosses the equator (the mean local time) precesses (shifts backwards) due to principles of orbital mechanics that are beyond the scope of this study. The earlier it gets the less useful the satellite becomes for science because the light levels become insufficient for proper imaging. The EO-1 satellite is projected to run out of maneuvering fuel in October 2011. The EO-1 research team will propose FY12 and FY13 funding to the NASA Senior Review, since even out of fuel, EO-1 can continue imaging for over a year before the mean local time precesses earlier than 9:45AM and it could take almost 2 years for it to go to 9:30. Even under the best circumstances, NASA will decommission EO-1 about 30 September 2013. A decadal survey mission called HypSPIRI is the follow on, but it may not launch until about 2022 or later. In the meantime, the EO-1 team at the Goddard Space Flight Center will propose a three satellite constellation hyperspectral to the EV-2 call (Venture class missions). If a positive response is received, it could be built starting about this time next year, and could be on-orbit before the decommissioning of EO-1, providing daily repeat of a 30 km swath of any point on the earth (Frye, 2010c). If all goes well, this new replacement suite will continue to provide a hyperspectral capability for archaeologists to use, which will greatly expand our abilities to conduct archaeological remote sensing studies over large areas.

paper and made helpful suggestions. Any failure to take their excellent advice is ours. Part of this research was supported by NSF IGERT Award #DGE-0966375, “Training, Research and Education in Engineering for cultural Heritage Diagnostics” at UC San Diego. Thanks to Ramesh Rao, Director, Calit2 San Diego Division; Ziad al-Saad, former Director General, Department of Antiquities of Jordan; Mohammad Najjar, UCSD Levantine Archaeology Lab.

References

- Adams, R. B. 1991. The Wadi Fidan project, Jordan, (1989). *Levant* XXIII:181–186.
- Alexakis, D., Sarris, A., Astaras, T., Albanakis, K., 2009. Detection of Neolithic settlements in Thessaly (Greece) through multispectral and hyperspectral satellite imagery. *Sensors* 9, 1167–1187.
- Barker, G., Gilbertson, D., Mattingly, D. (Eds.), 2007. *Archaeology and Desertification - The Wadi Faynan Landscape Survey*. Council for British Research in the Levant and Oxbow Books, Southern Jordan. Oxford.
- Ben-Yosef, E., Levy, T.E., Higham, T., Najjar, M., Tauxe, L., 2010. The beginning of Iron Age copper production in the southern Levant: new evidence from Khirbat al-Jariya, Faynan. *Antiquity* 84, 724–746.
- Ben-Yosef, E., Levy, T.E., Najjar, M., 2009. New iron age copper-mine fields discovered in southern Jordan. *Near Eastern Archaeology* 72, 98–101.
- Chavez, Pat S., 1988. An improved dark-object subtraction technique for atmospheric scattering correction of multispectral data. *Remote Sensing of Environment* 24, 459–479.
- Clark, R.N., Swayze, G.A., Wise, R., Livo, E., Hoefen, T., Kokaly, R., Sutley, S.J., 2007. USGS Digital Spectral Library splib06a. In: *Digital Data Series 231*. U.S. Geological Survey. <http://speclab.cr.usgs.gov/spectral.lib06/> Available online at.
- Conrad, H.G., Rothenberg, B. (Eds.), 1980. *Antikes Kupfer im Timna-Tal*. Deutsches Bergbau Museum, Bochum.
- Deroin, J., Téreygeol, F., Heckes, J., 2011. Evaluation of very high to medium resolution multispectral satellite imagery for geoarchaeology in arid regions – case study from Jabali, Yemen. *Journal of Archaeological Science* 38 (2011), 101–114.
- Finkelstein, I., 2005. Khirbat en-Nahas, Edom and Biblical History. *Tel Aviv* 32, 119–125.
- Finkelstein, I., Piasezky, E., 2006. 14C and the iron age chronology debate: Rehov, Khirbat en-Nahas, Dan and Megiddo. *Radiocarbon* 48, 373–386.
- Finkelstein, I., Piasezky, E., 2008. Radiocarbon and the History of Copper Production at Khirbat en-Nahas. *Tel Aviv* 35, 82–95.
- Finkelstein, I., Singer-Avitz, L., 2009. The pottery of Khirbat en-Nahas: a rejoinder. *Palestine Exploration Quarterly* 141, 207–218.
- Forté, M., 2010. *Cyber-Archaeology*. In: *BAR International Series 2177*. Archaeopress, Oxford.
- Frank, F., 1934. *Aus der Araba I: Reiseberichte*. Zeitschrift des Deutschen Palaestina Vereins 57, 191–280.
- Fritz, V., 1994. Vorbericht über die Grabungen in Barqa el-Hetiye im Gebiet von Fenan, Wadi el-Araba (Jordanien) 1990. *Zeitschrift des Deutschen Palaestina-Vereins* 110 (2), 125–150.
- Fritz, V., 1996. Ergebnisse einer Sondage in Hirbet en-Nahas, Wadi el-Araba (Jordanien). *Zeitschrift des Deutschen Palaestina Vereins* 112, 1–9.
- Frye, S. (2010a). NASA/Goddard Space Flight Center, Greenbelt, MD 20771, personal communication, July 13, 2010.
- Frye, S. (2010b). NASA/Goddard Space Flight Center, Greenbelt, MD 20771, personal communication, September 30, 2010.
- Frye, S. (2010c). NASA/Goddard Space Flight Center, Greenbelt, MD 20771, personal communication received October 14, 2010.
- Glueck, N., 1935. Explorations in Eastern Palestine, II. In: *Annual of the American Schools of Oriental Research*, vol. 15. American Schools of Oriental Research, New Haven. 1–288.
- Goodenough, D.A., Dyk, K., Niemann, J., Pearlman, H., Chen, T., Han, M., Murdoch West, C., 2003. Processing Hyperion and ALI for Forest classification. *IEEE Transactions on Geoscience and Remote Sensing* 41 (6), 1321–1331.
- Grattan, J.P., Gilbertson, D.D., Hunt, C.O., 2007. The local and global dimensions of metalliferous pollution derived from a reconstruction of an eight thousand year record of copper smelting and mining at a desert-mountain frontier in southern Jordan. *Journal of Archaeological Science* 34, 83–110.
- Hauptmann, A., 2007. *The Archaeo-metallurgy of Copper - Evidence from Faynan*. Jordan. Springer, New York.
- Higham, T., van der Plicht, J., Bronk Ramsey, C., Bruins, H.J., Robinson, M., Levy, T.E., 2005. In: Levy, T.E., Higham, T. (Eds.), *Radiocarbon dating of the Khirbat-en Nahas site (Jordan) and Bayesian modeling of the results*, in *The Bible and Radiocarbon Dating - Archaeology, Text and Science*. Equinox, London, pp. 164–178.
- Jupp, David L.B., 2001. *Discussion Around Hyperion Data*. Office of Space Science & Applications Earth Observation Centre, Canberra.
- Knabb, K., T. E. Levy, M. Najjar, and I.W.N. Jones. (in press). “Patterns of Iron Age Mining and Iron Age Settlement in Jordan’s Faynan district – the Wadi Al-Jariya Survey in Context.” in *New Insights into the Iron Age Archaeology of Edom, Southern Jordan - Surveys, Excavations and Research from the Edom Lowlands Regional Archaeology Project(ELRAP) 2006-2008*. Edited by T. E. Levy, E. Ben-Yosef, and M. Najjar. Boston: Annual of the American Schools of Oriental Research.

- Khurshid, K.S., Staenz, K., Sun, L., Neville, R., White, H.P., Bannari, A., Champagne, C.M., Hitchcock, R., 2006. Preprocessing of EO-1 Hyperion data. *Canadian Journal of Remote Sensing* 32 (2), 84–97.
- Kwong, J.D., Messinger, D.W., Middleton, W.D., 2009. Hyperspectral Clustering and Unmixing for Studying the Ecology of State Formation and Complex Societies Imaging Spectrometry XIV.
- Lehmann, B., 2008. The Archaeometallurgy of Copper. Evidence from Faynan, Jordan. Andreas Hauptmann, p. 388. Springer, Berlin-Heidelberg-New York, ISBN 978-3-540-72237-3. *Economic Geology* 103(2): 456–457.
- Levy, T.E., 2005. Grand Narratives, technological Revolutions and the Past: deep-time studies of metallurgy and social Evolution in the Eastern Mediterranean. In: La Bianca, O., Scham, S. (Eds.), *Connectivity in Antiquity - Globalization as a Long-Term Historical Process*. Equinox, London, pp. 10–26.
- Levy, T.E., 2008. Ethnic identity in biblical Edom, Israel and Midian: some insights from mortuary contexts in the lowlands of Edom. In: Schloen, D. (Ed.), *Exploring the Longue Durée: Essays in Honor of Lawrence E. Stager*. Eisenbrauns, Winona Lake, Ind., pp. 251–261.
- Levy, T.E., 2009. Pastoral nomads and iron age metal production in ancient Edom. In: Szuchman, J. (Ed.), *Nomads, Tribes, and the State in the Ancient Near East*. University of Chicago Press, Chicago, pp. 147–176.
- Levy, T.E., 2010. The new pragmatism: integrating anthropological, digital, and historical biblical archaeologies. In: Levy, T.E. (Ed.), *Historical Biblical Archaeology and the Future - The New Pragmatism*. Equinox, London, pp. 3–44.
- Levy, T.E., Adams, R.B., Anderson, J.D., Najjar, N., Smith, N., Arbel, Y., Soderbaum, L., Muniz, M., 2003. An iron Age landscape in the Edomite Lowlands: archaeological surveys along Wadi al-Ghuwayb and Wadi al-Jariya, Jabal Hamrat Fidan, Jordan, 2002. *Annual of the Department of Antiquities Jordan* 47, 247–277.
- Levy, T.E., Adams, R.B., Najjar, M., Hauptmann, A., Anderson, J.A., Brandl, B., Robinson, M., Higham, T., 2004. Reassessing the chronology of Biblical Edom: new excavations and 14C dates from Khirbat en-Nahas (Jordan). *Antiquity* 78, 863–876.
- Levy, T. E., Ben-Yosef, and M. Najjar. (in press). "New perspectives on iron age copper production and Society in the Faynan region, Jordan," in *Eastern Mediterranean Metallurgy and Metalwork in the 2nd Millennium BC*. Edited by V. Kassianidou and G. Pappasavvas. Oxford: Oxbow Books.
- Levy, T.E., Higham, T. (Eds.), 2005a. *The Bible and Radiocarbon Dating - Archaeology, Text and Science*. Equinox, London.
- Levy, T.E., Higham, T., 2005b. Radiocarbon dating and the Iron Age of the southern Levant: problems and potentials for the Oxford Conference. In: Levy, T.E., Higham, T. (Eds.), *The Bible and Radiocarbon Dating - Archaeology, Text and Science*. Equinox, London, pp. 3–14.
- Levy, T.E., Higham, T., Bronk Ramsey, C., Smith, N.G., Ben-Yosef, E., Robinson, M., Münger, S., Knabb, K., Schulze, J.P., Najjar, M., Tauxe, L., 2008. High-precision radiocarbon dating and historical biblical archaeology in southern Jordan. *Proceedings of the National Academy of Sciences* 105, 16460–16465.
- Levy, T.E., Najjar, M., 2006. Some thoughts on Khirbat en-Nahas, Edom, biblical history and anthropology - a response to Israel Finkelstein. *Tel Aviv* 33, 107–122.
- Levy, T.E., Najjar, M., Higham, T., 2005a. In: Bienkowski, P., van der Steen, E. (Eds.), *How Many Fortresses do you Need to Write a Preliminary Report? Or response to Edom and the Early Iron Age: Review of a Recent Publication in Antiquity*. University of Manchester, Manchester. <http://www.wadiarabahproject.man.ac.uk/>.
- Levy, T.E., Najjar, M., van der Plicht, J., Smith, N.G., Bruins, H.J., Higham, T., 2005b. Lowland Edom and the high and low chronologies: Edomite State formation, the Bible and recent archaeological research in southern Jordan. In: Levy, T.E., Higham, T. (Eds.), *The Bible and Radiocarbon Dating - Archaeology, Text and Science*. Equinox Publishing Ltd, London, pp. 129–163.
- Levy, T.E., Petrovic, V., Wypych, T., Gidding, A., Knabb, K., Hernandez, D., Smith, N.G., Schlulz, J.P., Savage, S.H., Kuester, F., Ben-Yosef, E., Buitenhuis, C., Barrett, C.J., Najjar, M., DeFanti, T., 2010. On-site digital archaeology 3.0 and cyber-archaeology: into the future of the past - new developments, delivery and the creation of a data avalanche. In: Forte, M. (Ed.), *Introduction to Cyber-Archaeology*. Archaeopress, Oxford, pp. 135–153.
- Lillesand, T., Keifer, R., Chipman, J., 2008. *Remote Sensing and Image Interpretation*, sixth ed. John Wiley & Sons, Hoboken.
- MacDonald, B., 1992. *The Southern Ghors and Northeast 'Arabah Archaeological Survey*. In: *Sheffield Archaeological Monographs*, vol. 5. J.R. Collis Publications, Sheffield.
- Mattingly, D., Newson, P., Grattan, J., Tomber, R., Barker, G., Gilbertson, D., Hunt, C., 2007. In: Barker, G., Gilbertson, D., Mattingly, D. (Eds.), *The Making of Early States: The Iron Age and Nabatean periods*, in *Archaeology and Desertification - The Wadi Faynan Landscape Survey, Southern Jordan*. Wadi Faynan Series, vol. 2. Oxbow Books, Oxford, pp. 271–303.
- Moersch, J.E., Christensen, P.R., 1995. Thermal emission from particulate surfaces: a comparison of scattering models with measured spectra. *Journal of Geophysical Research* 100 (4), 7465–7477.
- Musil, A., 1907. *Arabia Petraea*. I. Moab; II. Edom. Alfred Holder, Topographische Reisebericht. Wien.
- Parcak, Sarah H., 2009. *Satellite Remote Sensing for Archaeology*. Routledge, New York.
- Pearlman, Jay S., 2003. *Hyperion Validation Report*. Boeing Report Number 03-ANCOS-001. NASA/Goddard Space Flight Center, Greenbelt, MD.
- Pryce, T., Abrams, M., 2010. Direct detection of Southeast Asian smelting sites by ASTER remote sensing imagery: technical issues and future perspectives. *Journal of Archaeological Science* 37 (2010), 3091–3098.
- Pyatt, F.B., Barker, G.W., Birch, P., Gilbertson, D.D., Grattan, J.P., Mattingly, D.J.A., 1999. King Solomon's miners - starvation and bioaccumulation? An environmental archaeological investigation in southern Jordan. *Ecotoxicology & Environmental Safety* 43, 305–308.
- Rabb'a, I., 1994. Geological of the Al Qurayqira (Jabal Hamra Faddan area). Map Sheet No. 305111. 1:50,000. In: *Geological Mapping Series Geological Bulletin No 28*. Geology Directorate, Department of Natural Resources, Amman.
- Raikes, T., 1980. Notes on some Neolithic and later sites in Wadi Araba and the Dead Sea valley. *Levant* 12, 40–60.
- Ramsey, M.S., Christensen, P.R., 1998. Mineral abundance determination: quantitative deconvolution of thermal emission spectra. *Journal of Geophysical Research* 103, 577–596.
- Rothenberg, B., 1999. *Archaeo-metallurgical researches in the southern Arabah 1959-1990. Part 2: Egyptian new kingdom (Ramesside) to early Islam*. *Palestine Exploration Quarterly* 131, 149–175.
- Salisbury, J.W., Wald, A., 1992. The role of volume scattering in reducing spectral contrast of restraints bands in spectra of powdered minerals. *Icarus* 96, 121–128.
- Segev, A., Sass, E., 1989. in *geological Association of Canada Special paper 36*. In: Boyle, R., Brown, A.C., Jefferson, C.W., Jowett, E.C., Kirkham, R.V. (Eds.), *Copper-enriched syngenetic dolostones as a source for Epigenetic copper mineralization in sandstones and shales (Timna, Israel)*. Geological Association of Canada, Newfoundland.
- Traviglia, A., 2006. Archaeological usability of hyperspectral images: successes and failures of image processing techniques. December 4-7, 2006, Rome. In: Campana, S., Forte, M. (Eds.), *From Space to Place: Proceedings of the 2nd International Conference on Remote Sensing in Archaeology*. BAR International Series 1568. Archaeopress, Oxford, pp. 123–130.
- Ungar, Stephen G., 2010. *NASA/Goddard Space Flight Center, Greenbelt, MD 20771*, personal communication, October 17, 2010.
- Ungar, Stephen G., Pearlman, Jay S., Mendenhall, Jeffrey A., Reuter, Dennis, 2003. Overview of the earth observing one (EO-1) mission. *IEEE Transactions on Geoscience and Remote Sensing* 41 (6), 1149–1159.
- van der Steen, E., Bienkowski, P., 2006. Radiocarbon dates from Khirbat en-Nahas: a methodological critique. *Antiquity* 80, 1–3.
- Vincent, R.K., Beck, R.A., 2005. *Spectral Ratio Imaging with Hyperion Satellite Data for Geological Mapping*. Final Report, NASA Grant Number NCC 3-1093. http://ntrs.nasa.gov/archive/nasa/casi.ntrs.nasa.gov/20050159702_2005159675.pdf.